Global Journal of Engineering and Technology Advances

eISSN: 2582-5003

Cross Ref DOI: 10.30574/gjeta

Journal homepage: https://gjeta.com/

(RESEARCH ARTICLE)

Check for updates

Spatial deformations and transverse vibrations in the cutting mechanisms of big band saw machines: Investigation and analysis

Boycho Marinov *

Institute of Mechanics, Bulgarian Academy of Sciences, Bulgaria.

Global Journal of Engineering and Technology Advances, 2022, 13(03), 096–109

Publication history: Received on 14 November 2022; revised on 24 December 2022; accepted on 26 December 2022

Article DOI: https://doi.org/10.30574/gjeta.2022.13.3.0211

Abstract

In this paper, the influence of static and dynamic loads on the cutting mechanisms of big band saw machines is analyzed. For this purpose, functions describing the static deformations of the upper shaft in two mutually perpendicular planes were obtained. The influence of dynamic loads is also analyzed. In this case, the transverse vibrations and the dynamic deformations are studied. Functions describing the vibrations and deformations of the upper shaft have been received. Diagrams showing the type of elastic lines from static loading are built. Diagrams and surfaces, showing the type of the dynamic deformations are also built. The proposed theoretical expressions, diagrams and surfaces can be used to design new band saw machines, as well as to study the influence of various dynamic processes on the operation of machines in operating mode.

Keywords: Band saw machines; Elastic line; Transverse vibrations; Spatial deformations

1. Introduction

The band saw machines are a certain class of woodworking machines that are used in various technological processes of the woodworking industry. According to the diameters of the leading wheels and the width of the band saw blade, the band saw machines are divided into different groups. Of particular interest are the big band saw machines. These machines are used for sawing logs with very large diameters. As a result, very big loads occur during operation [1-3]. These loads cause large deformations in the main links of the machines.

The main purpose of this investigation is to study the influence of static and dynamic loads on the upper shaft of big band saw machines when the leading wheel is mounted at the end of the shaft.

To achieve this purpose, the following main tasks must be solved:

- investigation of upper shaft deformations as a result of static loads;
- investigation of the transverse vibrations and deformations of the upper shaft as a result of dynamic loads;
- construction of plane and spatial diagrams showing the change of the deformations of the upper shaft when changing different parameters.

2. Expose

In this part, the scheme of the cutting mechanism and the corresponding dynamic model are presented. They are used in order to solve the problems posed.

* Corresponding author: Boycho Marinov

2.1. Scheme of the cutting mechanism

The scheme of the cutting mechanisms is shown in Fig.1 [4,5]. The following symbols are defined: 1-main shaft, 2 and 5-belt pulleys, 3 and 4-leading wheels, *A* – band saw blade, and 6-upper shaft.

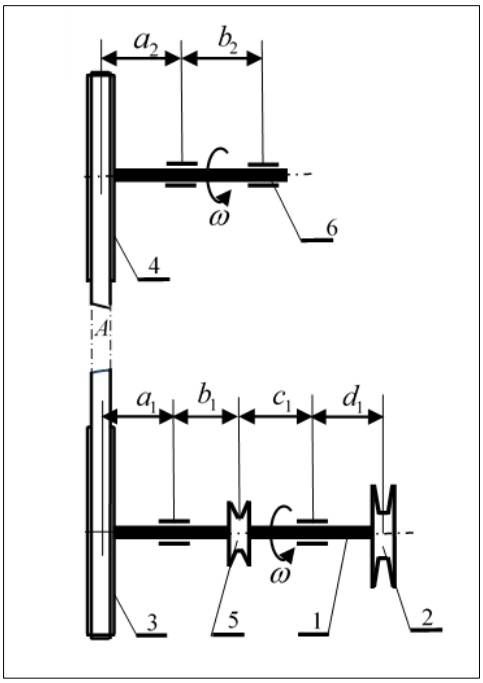

Figure 1 Cutting mechanism

2.2. Dynamic model

The upper leading wheel can be mounted on the shaft in two ways. The dynamic model showing the first way in which the leading wheel is mounted at the end of the shaft is shown in Fig. 2.

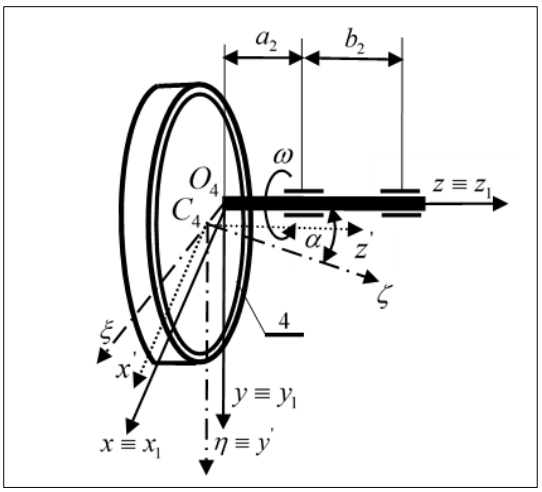

Figure 2 Dynamic model

The following coordinate systems are used to obtain expressions for calculating the full dynamic reactions [6]:

- O_4xyz - fixed coordinate system;
- $O_4x_1y_1z_1$ - moving coordinate system;
- $C_4x'y'z'$ - coordinate system, whose axes are parallel to the axes of the moving coordinate system;

- $C_4\xi\eta\zeta$ - coordinate system, whose axes are principal axes of inertia.

The linear deviation (eccentricity) e and angular deviation α are also shown in the figure as $e = O_4C_4$ and α is the angle between the axes ζ and z.

2.3. Static and dynamic loads on the upper shaft

The static and dynamic loads, as well as the full dynamic reactions have been determined by the author in his previous research [6]. They can be calculated from expressions (1).

$$K_x = K_x^{st} + K_x^d, \quad K_y = K_y^{st} + K_y^d,$$
$$L_x = L_x^{st} + L_x^d, \quad L_y = L_y^{st} + L_y^d. \qquad \text{.....(1)}$$

3. Deformations of the upper shaft as a result of static loads

We consider the static loads of the upper shaft in two mutually perpendicular planes, O_4yz and O_4xz. These loads are shown in Fig. 3.

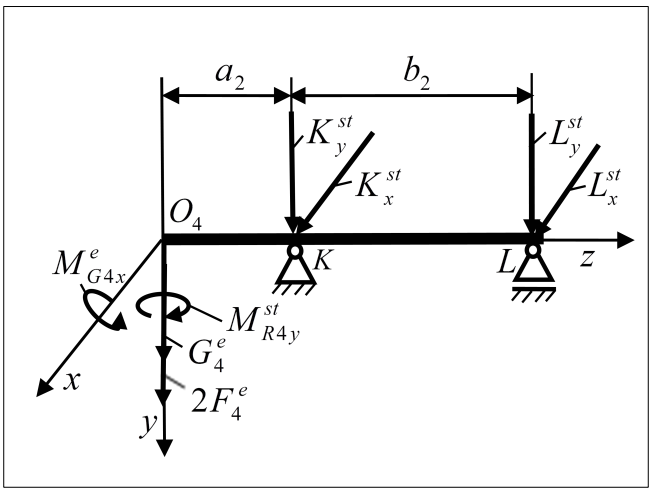

Figure 3 Static loads of the upper shaft

The static loads can be calculated from the following dependencies.

$$M_{G4x}^e = m_4 ge\sin\alpha, \quad M_{R4y}^{st} = \frac{1}{2}\left(\frac{mK_{\Delta(\lambda)}bHu}{V} + R_\Sigma\right)r_4\cos\alpha, \qquad \text{.....(2)}$$
$$G_4^e = m_4 g, \quad F_4^e = 1.5N_c/V,$$

where m_4 and r_4 are the mass and the radius of the leading wheel 4 and g is the acceleration of gravity. $K_{\Delta(\lambda)}$ is the specific work of the cutting [6-8]. R_Σ is the total resistance force. H is the thickness of the workpiece, u is the feeding speed, b is the width of the cutter, m is a coefficient ($0 \le m \le 1$). N_c is the cutting power and V is the cutting speed. The linear deviation (eccentricity) e and angular deviation α are shown in Fig.2 as $e = O_4C_4$ and α is the angle between the axes ζ and z. Static reactions are written below.

$$K_x^{st} = -\frac{r_4}{2b_2}\left(\frac{mK_{\Delta(\lambda)}bHu}{V} + R_\Sigma\right)\cos\alpha, \quad L_x^{st} = \frac{r_4}{2b_2}\left(\frac{mK_{\Delta(\lambda)}bHu}{V} + R_\Sigma\right)\cos\alpha,$$
$$K_y^{st} = -\frac{m_4 g}{b_2}(a_2 + b_2 + e\sin\alpha) - \frac{3N_c(a_2+b_2)}{b_2 V}, \quad L_y^{st} = \frac{m_4 g}{b_2}(a_2 + e\sin\alpha) + \frac{3N_c a_2}{b_2 V}. \qquad \text{.....(3)}$$

3.1. Static deformations in a vertical plane

To determine the static deformations, the following algorithm is used:

- Obtaining equations of the bending moments for each part of the shaft;
- Compilation of the differential equations of elastic lines;
- Obtaining expressions for determining the static deformations in a vertical plane for each part of the shaft.

The static loading in the vertical plane O_4yz is shown in Fig. 4.

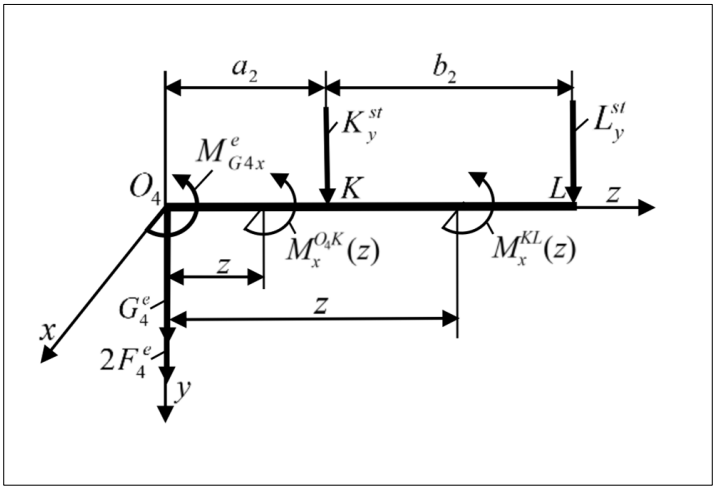

Figure 4 Static loads of the upper shaft in a vertical plane O_4yz

We apply the algorithm described above for this case of mounting the wheel.

- Part O_4K $\quad 0 \le z \le a_2$

$$M_x^{O_4K}(z) = -(G_4^e + 2F_4^e)z - M_{G4x}^e,$$
$$EJ_x y'' = (G_4^e + 2F_4^e)z + M_{G4x}^e, \qquad \text{.....(4)}$$
$$EJ_x y = \frac{(G_4^e + 2F_4^e)}{6}z^3 + \frac{M_{G4x}^e}{2}z^2 + K_1 z + L_1,$$

where E is the modulus of elasticity, J_x is the axial moment of inertia.

- Part KL $\quad a_2 \le z \le a_2 + b_2$

$$M_x^{KL}(z) = -(G_4^e + 2F_4^e + K_y^{st})z - M_{G4x}^e + K_y^{st}a_2,$$
$$EJ_x y'' = (G_4^e + 2F_4^e + K_y^{st})z + M_{G4x}^e - K_y^{st}a_2, \qquad \text{.....(5)}$$
$$EJ_x y = \frac{(G_4^e + 2F_4^e + K_y^{st})}{6}z^3 + \frac{(M_{G4x}^e - K_y^{st}a_2)}{2}z^2 + K_2 z + L_2.$$

The constants of integration $K_i, L_i\ (i=1,2)$ are determined by the boundary conditions. From these conditions, we obtain the following non-homogeneous algebraic system.

$$\begin{aligned}
&\frac{(G_4^e+2F_4^e)}{6}a_2^3+\frac{M_{G4x}^e}{2}a_2^2+K_1a_2+L_1=0,\\
&\frac{(G_4^e+2F_4^e+K_y^{st})}{6}a_2^3+\frac{(M_{G4x}^e-K_y^{st}a_2)}{2}a_2^2+K_2a_2+L_2=0,\\
&\frac{(G_4^e+2F_4^e)}{2}a_2^2+M_{G4x}^e a_2+K_1=\frac{(G_4^e+2F_4^e+K_y^{st})}{2}a_2^2+(M_{G4x}^e-K_y^{st}a_2)a_2+K_2,\\
&\frac{(G_4^e+2F_4^e+K_y^{st})}{6}(a_2+b_2)^3+\frac{(M_{G4x}^e-K_y^{st}a_2)}{2}(a_2+b_2)^2+K_2(a_2+b_2)+L_2=0.
\end{aligned} \qquad \text{.....(6)}$$

From the solution of this system, we get expressions for calculating the constants of integration in the final form.

$$\begin{aligned}
K_1&=-\frac{\left[3a_2(a_2+b_2)+b_2^2\right]\left(G_4^e+2F_4^e+K_y^{st}\right)}{6}-\frac{\left(2a_2+b_2\right)\left(M_{G4x}^e-K_y^{st}a_2\right)+K_y^{st}a_2^2}{2},\\
L_1&=\frac{a_2\left[3a_2(a_2+b_2)+b_2^2\right]\left(G_4^e+2F_4^e+K_y^{st}\right)}{6}+\frac{a_2(a_2+b_2)\left(M_{G4x}^e-K_y^{st}a_2\right)}{2}-\frac{a_2^3\left(G_4^e+2F_4^e\right)}{6},\\
K_2&=-\frac{\left[3a_2(a_2+b_2)+b_2^2\right]\left(G_4^e+2F_4^e+K_y^{st}\right)}{6}-\frac{\left(2a_2+b_2\right)\left(M_{G4x}^e-K_y^{st}a_2\right)}{2},\\
L_2&=\frac{a_2(a_2+b_2)(2a_2+b_2)\left(G_4^e+2F_4^e+K_y^{st}\right)}{6}+\frac{a_2(a_2+b_2)\left(M_{G4x}^e-K_y^{st}a_2\right)}{2}.
\end{aligned} \qquad \text{..... (7)}$$

3.2. Static deformations in a horizontal plane

To determine the static deformations of the upper shaft in the horizontal plane O_4xz , we use Fig.5. The static load in this plane is shown in the same figure. In this case, the horizontal plane is rotated about the axis of rotation of an angle $\pi/2$.

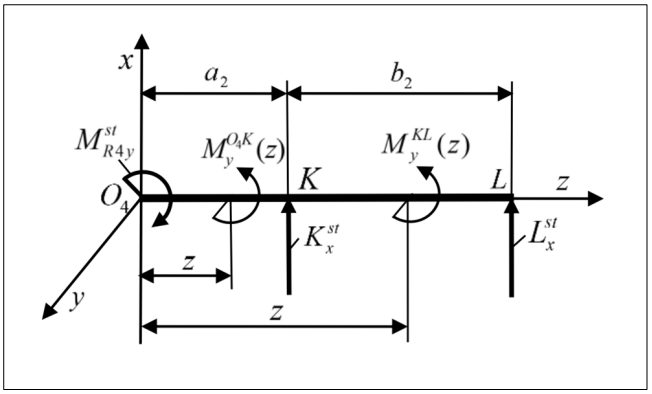

Figure 5 Static loads of the upper shaft in a horizontal plane O_4xz

In this case, we apply the algorithm described above.

3.2.1. Expressions for determining the static deformations in the horizontal plane O_4xz :

- Part O_4K $\quad 0 \le z \le a_2$

$$M_y^{O_4K}(z) = M_{R4y}^{st},$$
$$EJ_y x'' = M_{R4y}^{st}, \qquad \text{.....(8)}$$
$$EJ_y x = \frac{M_{R4y}^{st}}{2} z^2 + K_3 z + L_3.$$

where J_y is the axial moment of inertia.

- Part KL $\quad a_2 \le z \le a_2 + b_2$

$$M_y^{KL}(z) = K_x^{st} z + \left(M_{R4y}^{st} - K_x^{st} a_2\right),$$
$$EJ_y x'' = K_x^{st} z + \left(M_{R4y}^{st} - K_x^{st} a_2\right), \qquad \text{..... (9)}$$
$$EJ_y x = \frac{K_x^{st}}{6} z^3 + \frac{\left(M_{R4y}^{st} - K_x^{st} a_2\right)}{2} z^2 + K_4 z + L_4.$$

3.2.2. Non-homogeneous algebraic system:

$$\frac{M_{R4y}^{st}}{2} a_2^2 + K_3 a_2 + L_3 = 0,$$
$$\frac{K_x^{st}}{6} a_2^3 + \frac{(M_{R4y}^{st} - K_x^{st} a_2)}{2} a_2^2 + K_4 a_2 + L_4 = 0, \qquad \text{..... ..... (10)}$$

$$M_{R4y}^{st} a_2 + K_3 = \frac{K_x^{st}}{2} a_2^2 + (M_{R4y}^{st} - K_x^{st} a_2) a_2 + K_4,$$
$$\frac{K_x^{st}}{6} (a_2 + b_2)^3 + \frac{(M_{R4y}^{st} - K_x^{st} a_2)}{2} (a_2 + b_2)^2 + K_4 (a_2 + b_2) + L_4 = 0.$$

3.2.3. Expressions for calculating the constants of integration K_j, L_j $(j = 3,4)$ in final form:

$$K_3 = \frac{-3(2a_2 + b_2) M_{R4y}^{st} - b_2^2 K_x^{st}}{6}, \quad L_3 = \frac{3a_2 (a_2 + b_2) M_{R4y}^{st} + a_2 b_2^2 K_x^{st}}{6}, \qquad \text{.....(11)}$$

$$K_4 = \frac{\left(3a_2^2 - b_2^2\right) K_x^{st} - 3(2a_2 + b_2) M_{R4y}^{st}}{6}, \quad L_4 = \frac{a_2 \left(b_2^2 - a_2^2\right) K_x^{st} + 3a_2 (a_2 + b_2) M_{R4y}^{st}}{6}.$$

4. Deformations of the upper shaft as a result of dynamic loads

Dynamic deformations are caused by the loads that occur as a result of the inaccuracies with which the leading wheel is made. To determine these deformations, we use Fig. 6. This figure shows the dynamic reactions $K_x^d, K_y^d, L_x^d, L_y^d$ as well as the centrifugal forces Φ_{4x} and Φ_{4y} and the dynamic moments M_x^d and M_y^d that occur in the operating mode.

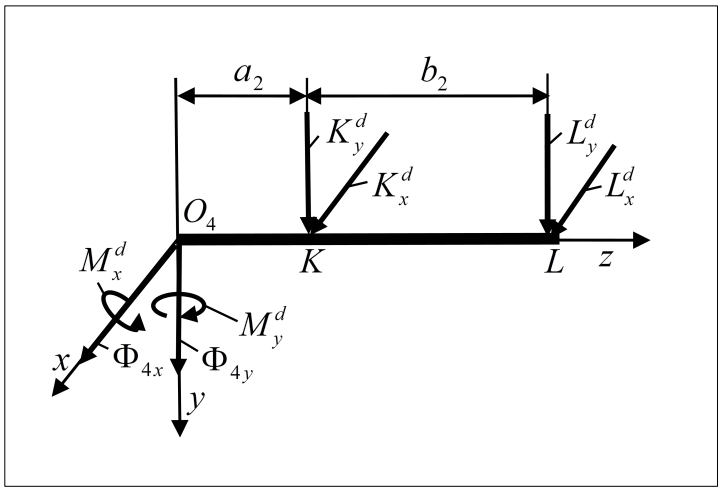

Figure 6 Dynamic loads of the upper shaft

The dynamic reactions can be written in the following form:

$$K_x^d = K_{bm}\cos\omega t, \quad K_y^d = K_{bm}\sin\omega t,$$
$$L_x^d = L_{bm}\cos\omega t, \quad L_y^d = L_{bm}\sin\omega t, \qquad \text{.....(12)}$$

where the amplitudes K_{bm} and L_{bm} are calculated from the following dependencies:

$$K_{bm} = -\frac{1}{2b_2}\left(\frac{mK_{\Delta(\lambda)}bHu}{V} + R_\Sigma\right)e\cos\alpha - \frac{\omega^2}{b_2}\left[(a_2 + b_2 + e\sin\alpha)m_4 e\cos\alpha - \frac{1}{2}\left(J_\xi - J_\zeta\right)\sin 2\alpha\right],$$

$$L_{bm} = \frac{1}{2b_2}\left(\frac{mK_{\Delta(\lambda)}bHu}{V} + R_\Sigma\right)e\cos\alpha + \frac{\omega^2}{b_2}\left[(a_2 + e\sin\alpha)m_4 e\cos\alpha - \frac{1}{2}\left(J_\xi - J_\zeta\right)\sin 2\alpha\right], \qquad \text{.....(13)}$$

where J_ξ and J_ζ are the mass moments of inertia of the leading wheel. The components of the centrifugal force Φ_{4x} and Φ_{4y} can be calculated from the following dependencies:

$$\Phi_{4x} = m_4\omega^2 e\cos\alpha\cos\omega t, \quad \Phi_{4y} = m_4\omega^2 e\cos\alpha\sin\omega t. \qquad \text{.....(14)}$$

The components of the dynamic moment M_x^d and M_y^d are shown in Fig. 6. These moments can be calculated from the dependencies (15).

$$M_x^d = M_{bm}\sin\omega t, \quad M_y^d = M_{bm}\cos\omega t, \qquad \text{.....(15)}$$

where

$$M_{bm} = \frac{1}{2}\left[\left(\frac{mK_{\Delta(\lambda)}bHu}{V} + R_\Sigma\right)e\cos\alpha - \omega^2\left(J_\xi - J_\varsigma - m_4 e^2\right)\sin 2\alpha\right].$$

4.1. Dynamic deformations in a vertical plane

In this part of the article, the dynamic deformations of the upper shaft in the vertical plane O_4yz are investigated. To solve this problem, we consider the shaft as a system having distributed mass. The inertial force Φ_{4y} and the moment M_x^d, written in expressions (14) and (15), act in this plane.

The differential equation of the transverse vibrations in this plane is written below [9].

$$\frac{EJ}{A_{ms}\rho}\frac{\partial^4 y}{\partial z^4}+\frac{\partial^2 y}{\partial t^2}=0, \quad \text{.....} \quad (16)$$

where E is the modulus of elasticity, $J=J_x=J_y$ is the axial moment of inertia, A_{ms} is the cross-sectional area of the shaft, ρ is the density of the material.

The solution of the differential equation (16) has the following form:

$$y_i(z,t)=Z_{2i}(z)\sin\omega t, \quad (i=1,2), \quad \text{.....} \quad (17)$$

where $Z_{2i}(z)$ is a function that depends on the *z* coordinate.

$$Z_{2i}(z)=\overline{K}_i\cos\omega_0 z+\overline{L}_i\sin\omega_0 z+\overline{M}_i ch\omega_0 z+\overline{N}_i sh\omega_0 z, \quad (i=1,2). \quad \text{.....} \quad (18)$$

In this expression ω_0 is a parameter $\left(\omega_0^4=A_{ms}\rho\omega^2/EJ\right)$ [9,5]. $\overline{K}_i,\overline{L}_i,\overline{M}_i,\overline{N}_i,(i=1,2)$ are constants of integration. They are determined by the boundary conditions for each part of shaft.

$$\begin{aligned}&\text{I. Part } O_4K \quad 0\le z\le a_2\\ &\text{II. Part KL} \quad a_2\le z\le a_2+b_2\end{aligned} \quad \text{.....} \quad (19)$$

In this case, we use four boundary conditions for each part of the shaft, so the boundary conditions for two parts will be eight in number. From these boundary conditions, we calculate the constants of integration. They are also eight in number, i.e., we obtain a non-homogeneous algebraic system with eight equations and eight unknown quantities. This algebraic system is written below.

$$\overline{N}_1-\overline{L}_1=\frac{m_4\omega^2 e\cos\alpha}{EJ\omega_0^3}, \quad \text{.....} \quad (20)$$

$$\overline{M}_1-\overline{K}_1=\frac{M_{bm}}{EJ\omega_0^2},$$

$$\overline{K}_1\cos\omega_0 a_2+\overline{L}_1\sin\omega_0 a_2+\overline{M}_1 ch\omega_0 a_2+\overline{N}_1 sh\omega_0 a_2=0,$$

$$\begin{aligned}&-\overline{K}_1\sin\omega_0 a_2+\overline{L}_1\cos\omega_0 a_2+\overline{M}_1 sh\omega_0 a_2+\overline{N}_1 ch\omega_0 a_2+\\ &\qquad \overline{K}_2\sin\omega_0 a_2-\overline{L}_2\cos\omega_0 a_2-\overline{M}_2 sh\omega_0 a_2-\overline{N}_2 ch\omega_0 a_2=0,\\ &-\overline{K}_1\sin\omega_0 a_2+\overline{L}_1\cos\omega_0 a_2-\overline{M}_1 sh\omega_0 a_2-\overline{N}_1 ch\omega_0 a_2+\\ &\qquad \overline{K}_2\sin\omega_0 a_2-\overline{L}_2\cos\omega_0 a_2+\overline{M}_2 sh\omega_0 a_2+\overline{N}_2 ch\omega_0 a_2=K_{bm}/EJ\omega_0^3,\end{aligned}$$

$$\overline{K}_2\cos\omega_0 a_2+\overline{L}_2\sin\omega_0 a_2+\overline{M}_2 ch\omega_0 a_2+\overline{N}_2 sh\omega_0 a_2=0,$$

$$\overline{K}_2\cos\omega_0(a_2+b_2)+\overline{L}_2\sin\omega_0(a_2+b_2)+\overline{M}_2 ch\omega_0(a_2+b_2)+\overline{N}_2 sh\omega_0(a_2+b_2)=0,$$
$$-\overline{K}_2\sin\omega_0(a_2+b_2)+\overline{L}_2\cos\omega_0(a_2+b_2)-\overline{M}_2 sh\omega_0(a_2+b_2)-\overline{N}_2 ch\omega_0(a_2+b_2)=L_{bm}/EJ\omega_0^3.$$

This system is presented below in matrix-vector form.

My=m ,..... (21)

where **M** is the basic matrix of the linear system. This matrix is obtained by the coefficients of the unknown variables and it has the following form.

M=..... (22)

$$\begin{bmatrix}
0 & -1 & 0 & 1 & 0 & 0 & 0 & 0\\
-1 & 0 & 1 & 0 & 0 & 0 & 0 & 0\\
\cos\omega_0 a_2 & \sin\omega_0 a_2 & ch\omega_0 a_2 & sh\omega_0 a_2 & 0 & 0 & 0 & 0\\
-\sin\omega_0 a_2 & \cos\omega_0 a_2 & sh\omega_0 a_2 & ch\omega_0 a_2 & \sin\omega_0 a_2 & -\cos\omega_0 a_2 & -sh\omega_0 a_2 & -ch\omega_0 a_2\\
-\sin\omega_0 a_2 & \cos\omega_0 a_2 & -sh\omega_0 a_2 & -ch\omega_0 a_2 & \sin\omega_0 a_2 & -\cos\omega_0 a_2 & sh\omega_0 a_2 & ch\omega_0 a_2\\
0 & 0 & 0 & 0 & \cos\omega_0 a_2 & \sin\omega_0 a_2 & ch\omega_0 a_2 & sh\omega_0 a_2\\
0 & 0 & 0 & 0 & \cos\omega_0(a_2+b_2) & \sin\omega_0(a_2+b_2) & ch\omega_0(a_2+b_2) & sh\omega_0(a_2+b_2)\\
0 & 0 & 0 & 0 & -\sin\omega_0(a_2+b_2) & \cos\omega_0(a_2+b_2) & -sh\omega_0(a_2+b_2) & -ch\omega_0(a_2+b_2)
\end{bmatrix}$$

y is a column vector. This vector is formed from the unknown constants of integration.

$$\mathbf{y}=\left[\overline{K}_1 \quad \overline{L}_1 \quad \overline{M}_1 \quad \overline{N}_1 \quad \overline{K}_2 \quad \overline{L}_2 \quad \overline{M}_2 \quad \overline{N}_2\right]^T. \text{.....} \quad (23)$$

m is a column vector. It is formed from the free members of the system.

$$\mathbf{m}=\left[\frac{m_4\omega^2 e\cos\alpha}{EJ\omega_0^3} \quad \frac{M_{bm}}{EJ\omega_0^2} \quad 0 \quad 0 \quad \frac{K_{bm}}{EJ\omega_0^3} \quad 0 \quad 0 \quad \frac{L_{bm}}{EJ\omega_0^3}\right]^T. \text{.....(24)}$$

The solutions of the non-homogeneous algebraic system (21) can be written as follows:

$$\overline{K}_i=\frac{\Delta_{\overline{K}_i}}{\Delta_M}, \quad \overline{L}_i=\frac{\Delta_{\overline{L}_i}}{\Delta_M}, \quad \overline{M}_i=\frac{\Delta_{\overline{M}_i}}{\Delta_M}, \quad \overline{N}_i=\frac{\Delta_{\overline{N}_i}}{\Delta_M}, \quad (i=1,2), \text{.....(25)}$$

where $\Delta_M=\det M$ is the determinant of the matrix **M**. This determinant is non-zero, because otherwise the mechanical system will operate in resonance mode.

The other determinants in expressions (25) are determinants of the matrices formed by the matrix **M**, in which the corresponding columns are replaced by the column vector **m** as follows:

$\Delta_{\overline{K}_i}$ $(i=1,2)$ – the first or fifth column of the matrix **M**,

$\Delta_{\overline{L}_i}$ $(i=1,2)$ – the second or sixth column of the matrix **M**,

$\Delta_{\overline{M}_i}$ $(i=1,2)$ – the third or seventh column of the matrix **M**,

$\Delta_{\overline{N}_i}$ $(i=1,2)$ – the fourth or eighth column of the matrix **M**.

For example, the determinant $\Delta_{\overline{K}_1}$ is written in the following way:

$$\Delta_{\overline{K}_1} = \text{..... (26)}$$

$$\begin{vmatrix}
\frac{m_4\omega^2 e\cos\alpha}{EJ\omega_0^3} & -1 & 0 & 1 & 0 & 0 & 0 & 0 \\
\frac{M_{bm}}{EJ\omega_0^2} & 0 & 1 & 0 & 0 & 0 & 0 & 0 \\
0 & \sin\omega_0 a_2 & ch\omega_0 a_2 & sh\omega_0 a_2 & 0 & 0 & 0 & 0 \\
0 & \cos\omega_0 a_2 & sh\omega_0 a_2 & ch\omega_0 a_2 & \sin\omega_0 a_2 & -\cos\omega_0 a_2 & -sh\omega_0 a_2 & -ch\omega_0 a_2 \\
\frac{K_{bm}}{EJ\omega_0^3} & \cos\omega_0 a_2 & -sh\omega_0 a_2 & -ch\omega_0 a_2 & \sin\omega_0 a_2 & -\cos\omega_0 a_2 & sh\omega_0 a_2 & ch\omega_0 a_2 \\
0 & 0 & 0 & 0 & \cos\omega_0 a_2 & \sin\omega_0 a_2 & ch\omega_0 a_2 & sh\omega_0 a_2 \\
0 & 0 & 0 & 0 & \cos\omega_0 (a_2+b_2) & \sin\omega_0 (a_2+b_2) & ch\omega_0 (a_2+b_2) & sh\omega_0 (a_2+b_2) \\
\frac{L_{bm}}{EJ\omega_0^3} & 0 & 0 & 0 & -\sin\omega_0 (a_2+b_2) & \cos\omega_0 (a_2+b_2) & -sh\omega_0 (a_2+b_2) & -ch\omega_0 (a_2+b_2)
\end{vmatrix}$$

We calculate the constants of integration $\overline{K}_i, \overline{L}_i, \overline{M}_i, \overline{N}_i, (i=1,2)$ using the dependencies (25). These constants are used to determine the functions $Z_{2i}(z), (i=1,2)$. The vertical displacements of the upper shaft are determined by the expressions (17). These expressions describe the displacements $y_i(z,t)$. The functions $Z_{2i}(z)$ take part in these expressions.

4.2. Dynamic deformations in a horizontal plane

The inertial force Φ_{4x} and the moment M_y^d, written in expressions (14) and (15), act in the horizontal plane O_4xz.

The differential equation of the transverse vibrations is written below [9]:

$$\frac{EJ}{A_{ms}\rho}\frac{\partial^4 x}{\partial z^4} + \frac{\partial^2 x}{\partial t^2} = 0. \text{ ..... (27)}$$

The symbols in this equation are explained in differential equation (16).

The solution of the above equation for each part of the shaft is written below.

$$x_i(z,t) = Z_{1i}(z)\cos\omega t, \quad (i=1,2), \text{ ..... (28)}$$

where $Z_{1i}(z)$ is a function that depends on the *z* coordinate.

$$Z_{1i}(z) = \overline{K}_j \cos\omega_0 z + \overline{L}_j \sin\omega_0 z + \overline{M}_j ch\omega_0 z + \overline{N}_j sh\omega_0 z, (j=i+2). \text{ ..... (29)}$$

$\overline{K}_j, \overline{L}_j, \overline{M}_j, \overline{N}_j, (j = i+2)$ are constants of integration that are determined by the boundary conditions for each part of shaft. These parts are described above in (19). And in this case, we obtain a non-homogeneous algebraic system. This algebraic system is written below.

$$\overline{N}_3 - \overline{L}_3 = \frac{m_4 \omega^2 e \cos\alpha}{EJ\omega_0^3}, \quad \text{(30)}$$

$$\overline{M}_3 - \overline{K}_3 = \frac{M_{bm}}{EJ\omega_0^2},$$

$$\overline{K}_3 \cos\omega_0 a_2 + \overline{L}_3 \sin\omega_0 a_2 + \overline{M}_3 ch\omega_0 a_2 + \overline{N}_3 sh\omega_0 a_2 = 0,$$

$$-\overline{K}_3 \sin\omega_0 a_2 + \overline{L}_3 \cos\omega_0 a_2 + \overline{M}_3 sh\omega_0 a_2 + \overline{N}_3 ch\omega_0 a_2 + \overline{K}_4 \sin\omega_0 a_2 - \overline{L}_4 \cos\omega_0 a_2 - \overline{M}_4 sh\omega_0 a_2 - \overline{N}_4 ch\omega_0 a_2 = 0,$$

$$-\overline{K}_3 \sin\omega_0 a_2 + \overline{L}_3 \cos\omega_0 a_2 - \overline{M}_3 sh\omega_0 a_2 - \overline{N}_3 ch\omega_0 a_2 + \overline{K}_4 \sin\omega_0 a_2 - \overline{L}_4 \cos\omega_0 a_2 + \overline{M}_4 sh\omega_0 a_2 + \overline{N}_4 ch\omega_0 a_2 = \frac{K_{bm}}{EJ\omega_0^3},$$

$$\overline{K}_4 \cos\omega_0 a_2 + \overline{L}_4 \sin\omega_0 a_2 + \overline{M}_4 ch\omega_0 a_2 + \overline{N}_4 sh\omega_0 a_2 = 0,$$

$$\overline{K}_4 \cos\omega_0 (a_2 + b_2) + \overline{L}_4 \sin\omega_0 (a_2 + b_2) + \overline{M}_4 ch\omega_0 (a_2 + b_2) + \overline{N}_4 sh\omega_0 (a_2 + b_2) = 0,$$

$$-\overline{K}_4 \sin\omega_0 (a_2 + b_2) + \overline{L}_4 \cos\omega_0 (a_2 + b_2) - \overline{M}_4 sh\omega_0 (a_2 + b_2) - \overline{N}_4 ch\omega_0 (a_2 + b_2) = \frac{L_{bm}}{EJ\omega_0^3}.$$

This non-homogeneous algebraic system is identical to the system recorded in (20). We can write the following equalities:

$$\overline{K}_3 = \overline{K}_1, \quad \overline{K}_4 = \overline{K}_2, \quad \overline{L}_3 = \overline{L}_1, \quad \overline{L}_4 = \overline{L}_2,$$
$$\overline{M}_3 = \overline{M}_1, \quad \overline{M}_4 = \overline{M}_2, \quad \overline{N}_3 = \overline{N}_1, \quad \overline{N}_4 = \overline{N}_2, \quad \text{(31)}$$

5. Numerical examples

The results of the carried out computer experiments are presented in Figs. 7÷9. We use initial data, presented in technical literature [8,10-12]:

5.1. Static deformations in vertical and horizontal planes

Figure 7 shows the deformations of the upper shaft in two mutually perpendicular planes. These deformations are caused by the static load.

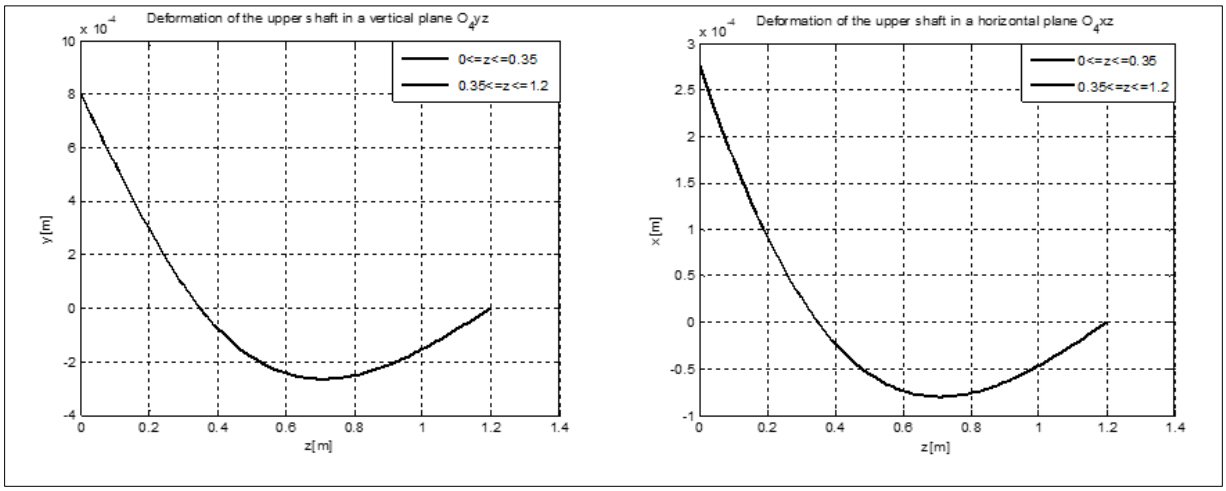

Figure 7 Deformations of the upper shaft in vertical and horizontal planes

These diagrams are drawn using the theoretical expressions obtained in the theoretical part of the article. The equations of the elastic lines are used. We can determine the type of elastic lines in both planes. Obviously they are continuous lines. It can also be seen that the deformations in the two supports are zero, i.e. when $z = 0.35[m]$ and $z = 1.2[m]$. We can also determine the most endangered cross section of the upper shaft. In the present case, the most endangered cross section is the initial cross section $(z = 0)$, as the static forces in this section are the largest.

5.2. Dynamic deformations in vertical and horizontal planes

Figure 8 shows the dynamic deformation of the upper shaft. We can see the deformations of the shaft in two different sections: $z = 0[m]$, $z = 0.775[m]$. These graphics are functions of the time t and they change by the harmonic law. We can also determine the amplitudes of the vibrations for the two cross-sections. The greatest deviation is in the initial section, where $z = 0$. This section is the most dangerous cross-section.

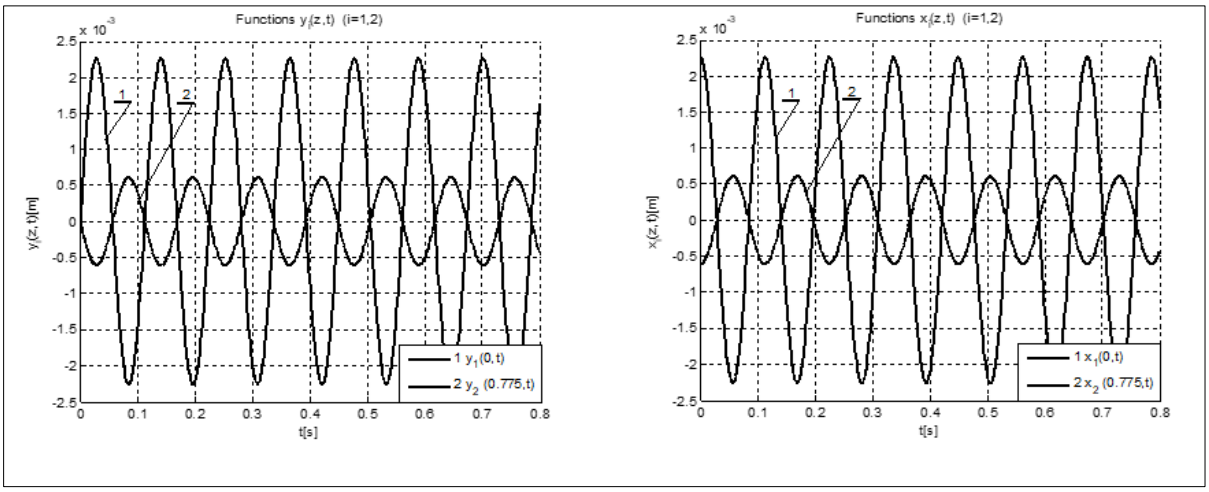

Figure 8 Dynamic deformations of the upper shaft in the planes O_4yz and O_4xz

Figure 9 shows the spatial deformations of the upper shaft.

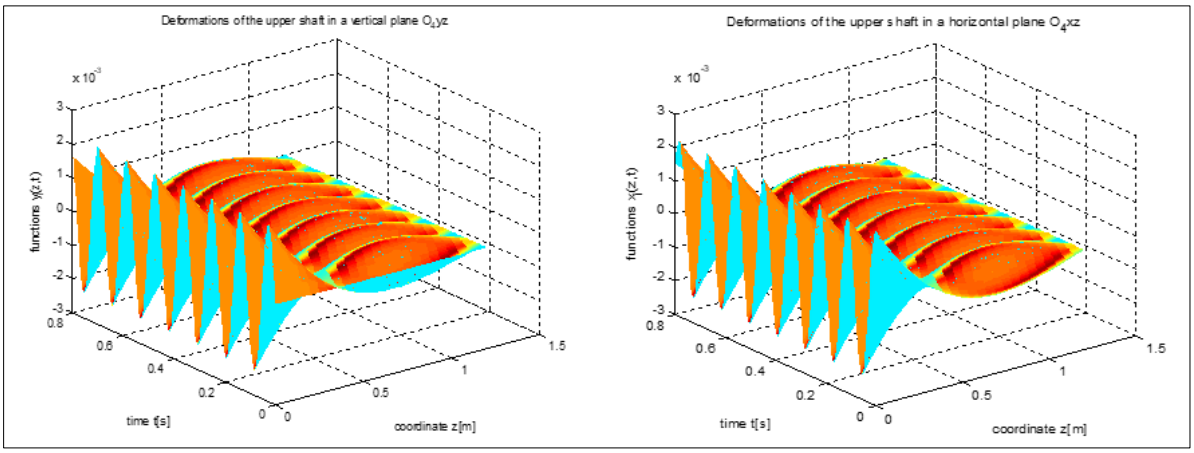

Figure 9 Upper shaft - deformations in a vertical and horizontal planes

These surfaces are built using the theoretical expressions obtained in this article. These expressions are the solutions of the differential equations describing the transverse vibrations of the shaft.

The following conclusions can be made after analyzing the presented surfaces:

- All cross section performs harmonic movement.
- The deformations in the two supports are equal to zero.
- The most endangered cross-section is the initial section of the shaft

6. Conclusion

In this paper, the influence of static and dynamic loads on the cutting mechanisms of big band saw machines is analised. For this purpose, dynamic model is built. Deformations of the upper shaft as a result of static loads are investigated. Theoretical expressions for calculating the static deformations of the shaft are obtained. The transverse vibrations of the upper shaft as a result of dynamic loads have been studied. Upper shaft deformations due to dynamic loads have also been studied. Theoretical expressions for calculating the dynamic deformations of the shaft when the leading wheel is mounted at the end of the shaft are obtained. Diagrams showing the type of elastic lines from static loading are built. Plane and spatial diagrams are drawn, showing the change of the deformations of the upper shaft when changing different parameters.

With the help of the obtained theoretical dependencies and diagrams different tasks can be solved by using known expressions from the technical literature. Some of the most important tasks are strength and deformation check of the shaft reduction of the shaft deformations, vibration control, achievement of minimum overall dimensions of the machines, etc.

Compliance with ethical standards

Acknowledgments

The author would like to express his acknowledgments to the Institute of Mechanics, Bulgarian Academy of Sciences, which is his workplace.

Disclosure of conflict of interest

The author of this article declares that he has no conflict of interest with anyone in conducting and completing this study.

References

[1] Hlásková L, Orlowski K, Kopecký Z, Jedinák M. Sawing processes as a way of determining fracture toughness and shear yield stresses of wood. BioResources. 2015; 10(3):5381-5394. doi:10.15376/biores.10.3.5381-5394.

[2] Moradpour P, Scholz F, Doosthoseini K, Tarmian A. Measurement of wood cutting forces during using piezoelectric dynamometer. Drvna industrija. 2016; 67(1):79-84. doi:10.5552/drind.2016.1433.

[3] Krenke T, Frybort S, Müller U. Determining cutting force parameters by applying a system function. Journal machining science and technology. 2017; 21(3):436-451. doi:org/10.1080/10910344.2017.1284563.

[4] Obreshkov P. Woodworking Machines. Publishing house "BM"; 1995.

[5] Marinov B. Dynamic and shock processes in some classes of woodworking machines. Analysis and optimization. Omniscriptum publishing group-Germany/LAP LAMBERT Academic publishing; 2018.

[6] Marinov B. Analytical and numerical determination of the full dynamic reactions in the bearing supports of big band saw machines. Journal of theoretical and applied mechanics. 2021; 51(4):488-501.

[7] Marinov B. Full dynamic reactions in the main links of big band saw machines. Global journal of engineering and technology advances. 2021; 9(3):92–104. https://doi.org/10.30574/gjeta.2021.9.3.0162.

[8] Gochev Zh. Handbook for exercise of wood cutting and woodworking tools. Publishing house in LTU; 2005.

[9] Cheshankov B. Theory of the vibrations. Publishing house of technical university – Sofia; 1992.

[10] Peters R. Band saw fundamentals: The complete guide. Hearst communications inc; 2006.

[11] Walker Turner. A comprehensive handbook on uses and applications of the band saw and jig saw. Literary licensing LLC; 2013.

[12] Barcík Š. Experimental cutting on the table band-sawing machine. European journal of wood and wood products. 2003; 61(4):313-320. doi:10.1007/s00107-002-0342-9.

[13] Dreizler R, Lüdde C. Theoretical mechanics: theoretical physics 1. Springer, Berlin, Heidelberg; 2010.doi:10.1007/978-3-642-11138-9.

[14] Dupen B. Applied strength of materials for engineering technology. Indiana university – Purdue university Fort Wayne; 2014.

[15] Chen Y, Wang X G, Sun C, Devine F. Active vibration control with state feedback in woodcutting. Journal of vibration and control. 2003; 9(6):645-664. https://doi.org/10.1177/1077546303009006002.